INVITED PAPER   *Special Section on EU's FP7 ICT R&D Project Activities on Future Broadband Access Technologies*

Anatomy of a Digital Coherent Receiver

Robert BORKOWSKI[†a)], **Darko ZIBAR**[†], *and* **Idelfonso TAFUR MONROY**[†], *Nonmembers*

SUMMARY   Digital coherent receivers have gained significant attention in the last decade. The reason for this is that coherent detection, along with digital signal processing (DSP) allows for substantial increase of the channel capacity by employing advanced detection techniques. In this paper, we first review coherent detection technique employed in the receiver as well as the required receiver structure. Subsequently, we describe the core part of the receiver — DSP algorithms — that are used for data processing. We cover all basic elements of a conventional coherent receiver DSP chain: deskew, orthonormaliation, chromatic dispersion compensation/nonlinear compensation, resampling and timing recovery, polarization demultiplexing and equalization, frequency and phase recovery, digital demodulation. We also describe novel subsystems of a digital coherent receiver: modulation format recognition and impairment mitigation via expectation maximization, which may gain popularity with increasing importance of autonomous networks.
key words: digital coherent receiver, coherent detection

1.   Introduction

Nowadays there is a paradigm shift in optical communications, where simple on-off keying (OOK) signalling is replaced by sophisticated methods utilizing coherent detection and digital signal processing. By encoding information in the amplitude, phase and polarization of the optical carrier considerably higher spectral efficiencies can be achieved.

The power of coherent detection coupled with capabilities of ultrafast digital signal processing (DSP) has allowed for revival of coherent optical communication with receivers based on electronic processing. Thanks to DSP, coherent optical communication systems operate closer to the nonlinear Shannon capacity limit by employing spectrally efficient modulation formats. Therefore, there is currently a lot of ongoing research on DSP algorithms for signal detection and optical fiber channel impairment compensation [1]. In more general terms, optical communication system are resembling their counterpart wireless communication. However, optical channel is different from wireless channel in terms of the length of the impulse response and also because the optical channel becomes nonlinear for increasing input power. Additionally, the baud rate of optical signals is much higher compared to the current wireless systems and this needs to be taken into account for the system design.

Linear signal processing algorithms from wireless communication can be effectively adapted to be used to compensate for linear fiber channel impairments and

have been demonstrated very successfully for higher order quadrature amplitude modulation (QAM) signaling [2]. However, for long-haul optical communication systems nonlinear optical fiber impairments can severely limit the transmission distance as well as the achievable total capacity [1].

Due to advances in electronics it became possible now to perform real-time implementations of very complex algorithm running at the required symbol rates, typically 28 Gbaud. For that reason, via this paper we would like to bring to the attention of the reader some novel ideas in the field of DSP for digital coherent receivers. Algorithms that a couple of years ago were infeasible to be implemented in DSP are slowly making its way to the market. With the emergence of dynamically switched network environments, such as CHRON architecture [3], advanced algorithms implemented directly in the integrated circuit of the receiver will gain importance.

In the subsequent sections of this paper we overview a generic architecture of a digital coherent receiver, along with basics of coherent detection. We then outline the DSP algorithms employed in a coherent receiver and include some of the new algorithms that may become part of a digital coherent receiver in future.

2.   Receiver Architecture

Industry representatives, through the Optical Internetworking Forum (OIF), have released an implementation agreement [4] outlining the most important physical, electrical and interface specifications of coherent receivers. This informal standard has been accepted by majority, if not all, manufacturers on the market. A generic outline of a digital coherent receiver, following the structure published by OIF, is shown in Fig. 1. It is composed of three major blocks: an optical front-end, an optoelectronic interface, and a DSP part. To enable coherent detection at current symbol rates, the DSP is implemented in a customized integrated circuit. One of the challenges for coherent receivers nowadays is the implementation of the entire receiver structure, including the optical front-end in a single photonic chip.

2.1   Optical Front-End

The optical front-end part is specified in the OIF agreement and is necessary to perform coherent detection.
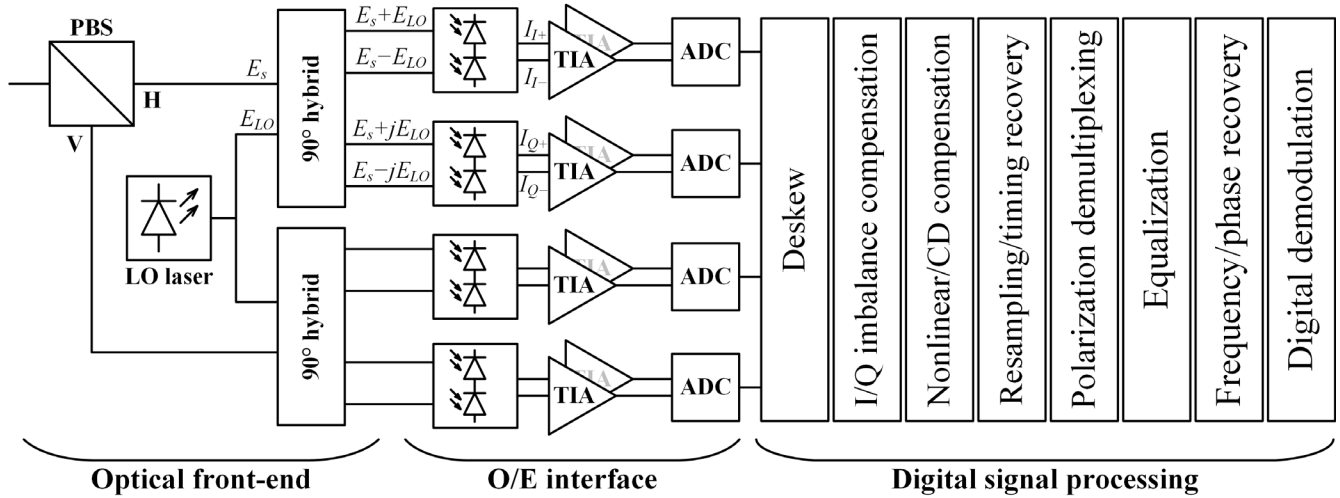
The remote signal carrying data is first split in two or-

Fig. 1 An outline of an optical digital coherent receiver. PBS — polarization beam splitter, LO — local oscillator, O/E — optical/electrical, TIA — transimpedance amplifier, ADC — analog-digital converter.

Table 1 Linewidth requirements for coherent detection [33].

Constellation	Max. tolerable $\Delta \nu \cdot \tau$ for 1 dB penalty @ BER = 10^{-3}	Max. tolerable $\Delta \nu$ for $\tau = 10\,Gbaud$
4-QAM	$4.1 \cdot 10^{-4}$	4.1 MHz
16-QAM	$1.4 \cdot 10^{-4}$	1.4 MHz
64-QAM	$4.0 \cdot 10^{-5}$	400 kHz
256-QAM	$8.0 \cdot 10^{-6}$	80 kHz

thogonal polarizations in a polarization beam splitter (PBS): horizontal — H, and vertical — V ($H \perp V$). Another laser, acting as a reference for the remote signal, necessary for coherent detection, is a local oscillator (LO). LO is split with a 3 dB coupler and carefully aligned as to match signal polarizations. Typically, both remote signal laser and local oscillator are either external cavity or fiber-based narrow linewidth laser in order to fulfill linewidth criteria given in Table 1.

Considering only one signal polarization, e.g. only H polarization in Fig. 1, as well as only one optical hybrid and two top balanced photodetectors, and assuming that fields have identical polarizations, the received signal can be written in scalar form as [5]

$$E_s(t) = \sqrt{P_s} \cdot e^{j(\omega_s t + \phi_s)} \cdot a(t) e^{j\phi(t)} \cdot e^{j\phi_{n_s}(t)}, \qquad (1)$$

where $a(t)$ and $\phi(t)$ represent time varying amplitude and phase of the data signal, and the LO signal is

$$E_{LO}(t) = \sqrt{P_{LO}} \cdot e^{j(\omega_{LO} t + \phi_{LO})} \cdot e^{j\phi_{n_{LO}}(t)}, \qquad (2)$$

where P_s and P_{LO} are powers of continuous wave (CW) signal, ω_s and $\omega_L O$ is the angular frequency ϕ_s and ϕ_{LO} initial phase, ϕ_{n_s} and $\phi_{n_{LO}}$ laser phase noise. The two signals are mixed in a 2×4 optical hybrid. Given inputs $E_s(t)$ and $E_{LO}(t)$, the optical hybrid output fields are

$$\frac{1}{2}(E_s(t) + E_{LO}(t))$$
$$\frac{1}{2}(E_s(t) + jE_{LO}(t))$$
$$\frac{1}{2}(E_s(t) - E_{LO}(t))$$
$$\frac{1}{2}(E_s(t) - jE_{LO}(t)).$$

First and third, as well as second and fourth hybrid outputs, form pairs. To enable coherent detection with differential output, each pair has to be detected by a balanced photodiode (cf. Fig. 1). For the first balanced photodetector the following currents result

$$I_{I+} = \frac{1}{2}R(E_s + E_{LO})^2 + i_{sh_1} =$$
$$= \frac{1}{2}RP_s \cdot a^2(t) + \frac{1}{2}RP_{LO} + i_{sh_1} +$$
$$+ R\sqrt{P_s P_{LO}} \cdot a(t) \cdot \cos\left[\Delta\omega t + \phi_n(t) + \phi_0 + \phi(t)\right], \qquad (3)$$

$$I_{I-} = \frac{1}{2}R(E_s - E_{LO})^2 + i_{sh_2} =$$
$$= \frac{1}{2}RP_s \cdot a^2(t) + \frac{1}{2}RP_{LO} + i_{sh_2} +$$
$$- R\sqrt{P_s P_{LO}} \cdot a(t) \cdot \cos\left[\Delta\omega t + \phi_n(t) + \phi_0 + \phi(t)\right], \qquad (4)$$

where i_{sh_1} and i_{sh_2} are the shot noise photocurrents, $\Delta\omega = \omega_s - \omega_{LO}$ is the angular frequency offset, $\phi_n(t) = \phi_{n_s}(t) - \phi_{n_{LO}}(t)$ is the total laser phase noise, and $\phi_0 = \phi_s - \phi_{LO}$ is the initial phase offset. Similarly for the second photodetector, two currents I_{Q+} and I_{Q-} are obtained except that $\cos(\cdot)$ in Eqs. (3) and (4) is replaced by $\sin(\cdot)$.

In a time interval τ, equal to the time symbol, the phase noise variance is given by

$$\left\langle \Delta\phi_n^2(\tau) \right\rangle = 2\pi \left(\Delta\nu_s + \Delta\nu_{LO}\right)\tau = 2\pi\Delta\nu\tau, \tag{5}$$

where $\Delta\nu = \Delta\nu_s + \Delta\nu_{LO}$ is the combined linewidth of the signal and LO laser. In Table 1 in Sect. 3.8 we list required values of $\Delta\nu\tau$ for various modulation formats.

The first two terms in Eqs. (3) and (4) are the direct detection terms of the signal and the LO power, where for coherent detection, typically $P_s \ll P_{LO}$. After balanced photodetection, those terms cancel out and only the beating is recovered

$$
\begin{aligned}
I_I(t) &= I_{I+} - I_{I-} \\
&= R\sqrt{P_s P_{LO}} \cdot a(t)\cdot \\
&\quad \cdot \cos\left[\Delta\omega t + \phi_n(t) + \phi_0 + \phi(t)\right] + i_{I_{sh}},
\end{aligned} \tag{6}
$$

$$
\begin{aligned}
I_Q(t) &= I_{Q+} - I_{Q-} \\
&= R\sqrt{P_s P_{LO}} \cdot a(t)\cdot \\
&\quad \cdot \sin\left[\Delta\omega t + \phi_n(t) + \phi_0 + \phi(t)\right] + i_{Q_{sh}},
\end{aligned} \tag{7}
$$

where i_{sh} is the total shot noise photocurrent for in-phase (subscript I) and quadrature (subscript Q) branch of the receiver. Clearly, $I_I(t) + jI_Q(t)$ is a complex number that linearly maps signal amplitude $a(t)$ and phase $\phi(t)$ into electrical domain. In this paper we consider heterodyne detection where $\Delta\omega \neq 0$, that is detected signal has a residual frequency offset not removed by beating.

2.2 Optical-Electrical Interface

The task of the optical-electrical (O/E) interface in a digital coherent receiver is to convert a signal carried in the optical field to digital domain. It is constituted by balanced photodetectors, transimpedance amplifiers (TIAs) and analog-digital converters (ADC). The task of the first is to detect outputs of the 90° hybrid. TIAs convert the photocurrents into a voltage signal. Subsequently ADC perform signal quantization and sampling, converting analog signal to a digital representation, thus preparing the signal for further electronic processing.

3. Digital Signal Processing Algorithms

The internal implementation of functionalities of the DSP part of the receiver is up to the system vendor.

3.1 Deskew

Signal arriving at the input of the digitizing circuit should be aligned in time to perform acquisition properly. For that reason, all paths in the receiver should ideally be phase matched. However, rough alignment, requiring delay in the order of number of samples, can be corrected in DSP by signal cross-correlation [2]. Sub-symbol time skew can be corrected by implementing hardware delay circuits or can be corrected in the follow-up DSP by interpolation.

3.2 I/Q Imbalance Compensation

By using a 90° optical hybrid, the received I and Q signals should be orthogonal to each other. In reality, imperfections of a transmitter, such as: incorrect bias point of a modulator, non-exact splitting ratios of couplers, misadjustments of polarization controllers; or of a receiver, in the optical hybrid, destroy orthogonality between I and Q channels, introducing quadrature imbalance. This in turn, leads to phase and amplitude errors in the received signal and thus degraded performance of a coherent optical communication systems. This detrimental effect is compensated in the DSP by applying orthonormalization of the received data [6]. A widely used approach involves Gram-Schmidt orthonormalization process, in which one vector is taken as a reference while the other is computed to orthogonalize the signal. This process is followed by normalizing the vector and thus signal power, to unity.

3.3 Chromatic Dispersion Compensation

The next step in the receiver is to compensate for chromatic dispersion. For practical purpose, dispersion transfer function can be well approximated by discarding terms of the Taylor-expanded propagation equation beyond the second. The transfer function H is then written as

$$H(L,R) = \exp\left(-jD\frac{\lambda^2}{c}\pi R^2 L\right), \tag{8}$$

where L is the fiber length, R is the symbol rate, D is the dispersion parameter, λ is wavelength and c speed of light. Standard method to compensate the dispersion is to pass the time domain signal through an finite impulse response filter structure [7]. However, the number of complex multiplications that has to be performed in hardware increases linearly with the dispersion length. Therefore the most widespread approach, requiring substantially less multiplications, is to use frequency domain filtering. In this case, overlap-add or overlap-save method is used [8], where the signal is divided into overlapping blocks, each block is multiplied with a transfer function, as defined in Eq. (8), and then combined back into a dispersion-free signal. Typically, all parameters in Eq. (8), except for the product DL are known in advance, and are specific to given fiber-optic communication system. There exist a number of different algorithms for detecting chromatic dispersion value, by optimizing the dispersion-length product DL.

Those can be divided into non data-aided and data-aided, i.e., based on the use of training sequences. Since we are mostly interested in blind receivers, we will shortly review non data-aided algorithm, as many different approaches to this problem have been made. The conventional method is based on parameter extraction from equalizer taps [9]. Due to a limited number of filter taps in the receiver, this solution might only be used to monitor relatively small CD, roughly corresponding to a stretch of one fiber span in long

haul network. To support longer links, other methods, based on CD scanning are used. In those techniques, the space of possible CD values is searched in small steps (20–200 ps/nm [10]) and a metric value is computed for each step. A characteristic feature of this metric, often global minimum or maximum, is used to indicate successful mitigation of CD. Diverse variants of this procedure, each using a different metric, have been shown so far. A criterion derived from constant modulus algorithm (CMA) is used in [10], [11], delay-tap sampling estimator [12], [13], autocorrelation of signal power waveform [14], [15], clock tone search [16]–[18], Gardner time error detector variance [19]. Recently, another technique has been demonstrated, where the sweep over CD values is performed automatically when applying FFT on the autocorrelation of discrete spectrum [20].

3.4 Nonlinearities Compensation

Compensation of nonlinear effects via digital backpropagation (DP) [21] may be performed as an alternative to chromatic dispersion compensation. The idea behind DP is to jointly mitigate the dispersion as well as nonlinear impairments by numerically solving an inverse nonlinear Schrödinger equation through the fiber. This way, the received signal may be used to estimate the transmitted signal, given parameters of a fiber link. Formerly, DP was a task requiring large computational power and implementing it in the receiver DSP was infeasible due to very high complexity of calculations. With time, simplified algorithms have appeared making it possible to implement different versions of DP algorithms in the receivers' DSP.

3.5 Resampling and Timing Recovery

Typically ADC does not operate in sync with the transmitter. In practice, the number of acquired samples per symbol may be as low as 1.4 up to significant oversampling of 2.5 sample per symbol or more. After CD (CD with nonlinearities) has been compensated, it becomes possible to acquire correct symbol clock and symbol timing, as the subsequent subsystem typically operate at a symbol rate (one sample per symbol) or twice the symbol rate (two samples per symbol). The signal from the previous block is fed into a timing recovery loop. First, the signal is resampled in the interpolator, by using e.g. spline or cubic interpolation to two samples per symbol. Since the exact frequency as well as initial phase of the signal is not know, the sampling points are arbitrary. Subsequently, timing error estimator sets in, which generates an error function which increases with an increasing distance from the correct sampling point. A very widespread algorithm, which operates at two samples to accomplish this task was invented by Gardner [22]. The timing error estimator works in a loop with the interpolator and its output is used to correct for the mismatch between actual and correct sampling point.

An alternative solution to this problem is provided by early-late algorithm. This algorithm requires high oversam-

pling rate (at least 3 samples per symbols). The correct sampling instance is found by looking for a point with highest variance. Due to the required high oversampling rate, this algorithm is of little use for optical communications, where even the symbol frequency is at the edge of capabilities of electronics.

3.6 Stokes Space Processing

Developments within the field of digital signal processing (DSP) make it possible to shift away from conventional well-established DSP algorithms that were inherited after RF receiver. One reason is that optics possess some tools which are unique to the field. One of them are Stokes parameters represented in the Poincaré sphere. The signal undergoes a following transformation

$$\mathbf{S} = \begin{pmatrix} S_0 \\ S_1 \\ S_2 \\ S_3 \end{pmatrix} = \begin{pmatrix} |h|^2 + |v|^2 \\ |h|^2 - |v|^2 \\ 2\Re\{hv^*\} \\ 2\Im\{hv^*\} \end{pmatrix} \tag{9}$$

where (S_1, S_2, S_3) is treated as a vector of coordinates in a 3-dimensional (3D) space. With this representation polarization mixing, carrier frequency offset and phase offset do not affect the 3D representation of the signal in the Poincaré sphere. Stokes space representation of the signal, coupled with machine learning algorithms opens new possibilities for statistical signal processing. An example of application of these new method is well represented by a relatively novel subsystem, aimed at modulation format recognition (MFR) [23]. This subsystem implements variational Bayesian expectation maximization (VBEM) for Gaussian mixture models (GMM) [24] to detect and count the number of clusters in the Stokes space. This is shown in Fig. 2. As each modulation format (such as QPSK or 16-QAM) will exhibit a different fingerprint — number of clusters in the Stokes space, counting them will be equivalent to detecting the modulation format. The proposed method enabled a major improvement over the constellation analysis-based techniques, as it allows for MFR at a considerably earlier stage in the receiver. The method does not require training, in contrast to neural network-based solution. The information about recognized modulation format can be subsequently fed forward to the following DSP blocks to improve their performance.

Several algorithms implementing various functionalities of the receiver were developed to operate in Stokes space and are advantageous due to lower complexity or faster convergence. The array of algorithms operating in the Stokes space includes: polarization demultiplexing [25], [26], whose conventional version is described in Sect. 3.7, cross-polarization modulation compensation [27], PDL compensation [28] or OSNR monitoring [29].

3.7 Polarization Demultiplexing and Equalization

Chromatic dispersion compensation removes bulk of the im-
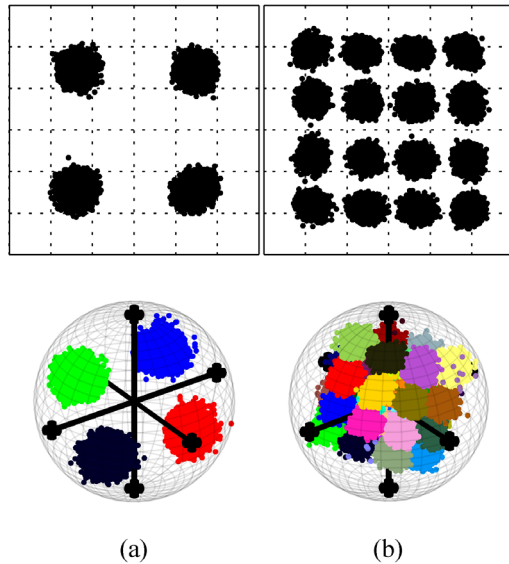
Fig. 2 Modulation format detection. Top row: constellation diagrams (after compensating for polarization mixing and frequency, and carrier offsets); bottom row: Stokes space representation of the corresponding signals (before compensating for the impairments). The data represented in Stokes space are not sensitive to the same impairments as the constellation representation.
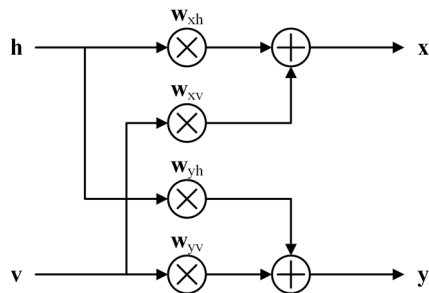
Fig. 3 Graphical representation of the polarization demultiplexing and equalization filter.

pairment related to chromatic dispersion. Even though advanced chromatic dispersion estimation algorithms are used [30], the amount compensated in CD compensation step may be off by as much as couple of hundred of ps/nm. To account for this residual CD, and to address other time varying impairments — particularly polarization mode dispersion (PMD) — another equalization stage is used. Typically, this equalization stage is at the same time compensating for polarization rotation. Signals $\mathbf{x}$ and $\mathbf{y}$ that originate at the transmitter in polarizations $X \perp Y$ are then incident on a receiver with orthogonal axes $H \perp Y$. Signals $\mathbf{h}$ and $\mathbf{v}$ constitute a mixture of $\mathbf{x}$ and $\mathbf{y}$. This process can be described by a following Jones matrix [31]

$$\begin{pmatrix} \mathbf{h} \\ \mathbf{v} \end{pmatrix} = \begin{pmatrix} \sqrt{\alpha}e^{j\delta} & -\sqrt{1-\alpha} \\ \sqrt{1-\alpha} & \sqrt{\alpha}e^{-j\delta} \end{pmatrix} \begin{pmatrix} \mathbf{x} \\ \mathbf{y} \end{pmatrix}, \qquad (10)$$

where α is a power splitting ratio depending on misalignment between $X \perp Y$ and $H \perp Y$, and δ is the phase difference between two polarization modes. Polarization de-

multiplexing is a process in which original transmitted signals $\mathbf{x}$ and $\mathbf{y}$ are extracted from received signals $\mathbf{h}$ and $\mathbf{v}$. Most commonly used method for polarization demultiplexing uses constant modulus algorithm (CMA) and has been described by Kikuchi [31] followed by an extensive analysis by Savory [2]. A finite impulse response filter for resolving polarization mixing is also providing signal equalization. The general structure of polarization demultiplexing filter (a 'butterfly filter') is presented in Fig. 3. This is a 2×2 multiple-input multiple-output filter described by the following equations

$$\begin{aligned} x &= \mathbf{w}_{xh}^H \mathbf{h} + \mathbf{w}_{xv}^H \mathbf{v} \\ y &= \mathbf{w}_{yh}^H \mathbf{h} + \mathbf{w}_{yv}^H \mathbf{v} \end{aligned} \qquad (11)$$

where $\mathbf{w}$ is an vector with filter tap weights for each specific input-output combination. In case where CMA is used, filter weights are adapted using a following error function that evaluates the distance of the received points from a unit circle

$$\begin{aligned} \varepsilon_x(n) &= R^2 - |x(n)|^2 \\ \varepsilon_y(n) &= R^2 - |y(n)|^2, \end{aligned} \qquad (12)$$

where $R = 1$. This adaptation is especially well suited for QPSK modulation format whose property is that, after normalization of average power to unity, all points lie on a unit circle. For higher-order modulation formats that are radially symmetric in I/Q plane, such as 16-QAM, multi-modulus algorithm (MMA), also called radially directed equalizer (RDE) may be used [2]. MMA is an extension of CMA in which the error function is a distance to the closest circle radius. For instance, 16-QAM has three radiuses, therefore, 12, after normalizing average signal power to 1, R can assume one of the following values $\left(1/\sqrt{5}, 1, 3/\sqrt{5}\right)$, where the closest one to the received data point is used.

A decision directed (DD) equalization, is similar, except for the fact that a reference constellation grid is used and the error function is evaluated as a distance between the received symbol and the closest point from a reference grid. DD equalization requires any frequency offset to be corrected before equalization. This calls a feedback from carrier recovery subsystem, described in the following section, to equalization subsystem. Often CMA or MMA is first used to preconverge the equalizer before DD mode, to avoid convergence problems (achieving local, instead of global minimum of the error function).

Regardless of the equalizer type employed, the following update equations for the equalizer weight are used

$$\begin{aligned} \mathbf{w}_{xh} &= \mathbf{w}_{xh} + \mu \varepsilon_x \mathbf{h} x^* \\ \mathbf{w}_{xv} &= \mathbf{w}_{xv} + \mu \varepsilon_x \mathbf{v} x^* \\ \mathbf{w}_{yh} &= \mathbf{w}_{yh} + \mu \varepsilon_y \mathbf{h} y^* \\ \mathbf{w}_{yv} &= \mathbf{w}_{yv} + \mu \varepsilon_y \mathbf{v} y^* \end{aligned} \qquad (13)$$

A problem observed with CMA is singularity, where due to blind filter weights update algorithm, taps converge

to a solution, where both recovered signals are the same, i.e. $\mathbf{x} = \mathbf{y}$ (possibly delayed wrt. each other). The other data signal is in this case discarded and treated as noise. This problem may be avoided by noting the fact that, neglecting CD and PMD, the transfer function of the optical system composed of rotators and retarders must be unitary [32]. Therefore, filter weights may be derived as $\mathbf{w}_{yh} = -\mathbf{w}_{xv}^*$ and $\mathbf{w}_{yv} = \mathbf{w}_{xh}^*$. In real systems, CD and PMD may not be disregarded, which renders singularity avoidance a serious issue, with many methods experimentally tested in [32].

Finally, a training sequence may be used to adapt the filter taps using e.g. least mean squares (LMS) algorithm.

3.8 Frequency and Phase Recovery

Frequency correction, or carrier recovery, subsystem is responsible for removing the residual frequency offset $\Delta\omega$ after heterodyne detection. In the received signal constellation, the residual frequency offset is seen as a progressing rotation of the constellation reference frame. Following that, the phase recovery removes the residual phase offset ϕ_0, which represent itself as a rotated constellation reference.

Robustness of the frequency and phase recovery subsystem against phase noise is critical for the performance of the receiver Because of large phase noise, the frequency recovery may fail by producing cycle slips or entirely losing synchronization, leaving the residual frequency offset incorrectly compensated. In Table 1, maximum combined linewidth requirements are presented for different constellation orders [33]. The presented numbers are, however very optimistic. Most often, when a conventional digital phase-locked loop (DPLL) [34] actual requirements may be one order of magnitude lower. DPLL has been found to work well for a wide range of QAM modulation formats, such as QPSK, 16-QAM and 64-QAM, provided that linewidth requirements are met.

Once the correct frequency offset $\Delta\omega$ is acquired by the DPLL, it is multiplied upon the signal to correct for it. As a next step, the residual phase offset has to be corrected. Very widespread method for phase offset correction was invented by Viterbi and Viterbi (V&V). The method is particularly suited for phase-shift keyed signals with m points [35]. The method uses the property of complex numbers, where m roots of a complex number raised to the power of m become the same number. The estimation is done on a block of sybmols $a[n]e^{j\phi[n]}$ of length N. For $m = 4$, the phase offset estimate $\hat{\theta}$ by which the received symbols have to be rotated is obtained as

$$\hat{\theta}[n] = \frac{1}{4}\arg\left\{\left(\frac{1}{N}\sum_{n=-N/2}^{N/2} a[n]e^{j\phi[n]}\right)^4\right\}, \qquad (14)$$

where $\arg(\cdot)$ is the argument of the complex number. This method, can be also used with higher order QAM signals [36] by partitioning them into distinct sets of QPSK constellations. It should be also noted that V&V algorithm may entirely replace traditional DPLL. To achieve this functionality, instead of running the algorithm on subsequent blocks, the estimation has to be performed over a sliding window. Average of differentials $\hat{\theta}[n + 1] - \hat{\theta}[n]$ will then result in the frequency offset.

3.9 Digital Demodulation

The last step in the receiver chain is to perform digital demodulation. The recovered data points are represented in an I/Q plane. A standard method of decoding the received data, for QAM systems, is by taking decisions based on a minimum Euclidean distance between the received point and one of the points of the reference constellation. This is hard decision based decoding. However, this method implicitly assumes that all transmitted symbols are equiprobable, have the same noise distribution, and that constellation does not undergo deformation. While the first is true due to precoding techniques, the latter two do not necessarily hold. An example of 16-QAM constellation affected only by additive white Gaussian noise is shown in Fig. 4(a). The distribution of noise in the constellation may change due to lasers phase noise or nonlinear impairments that depend on symbol power and data pattern. It can be observed in Fig. 4(b) that under influence of laser phase noise, outer constellation points become elliptical, while the inner points still maintain circular shape. Finally, in Fig. 4(c), a constellation affected by a nonlinear phase noise (NLPN) is shown. In this case, all the clusters loose their circular symmetry. Moreover, depending on the power (distance from the origin of the I/Q plane), they experience different frequency offsets and the entire constellation shape becomes malformed. To address this issues techniques such as k-means or expectation maximization (EM) can be used. k-means attempt to optimize the reference constellation grid to match the received signal by iteratively finding clusters' centroids. EM technique represents each constellation as a mixture of i.i.d. Gaussians with unknown means and covariances. An iterative process is used to optimize reference grid boundaries based on actual received data. These new methods have been successfully used to improve system performance in nonlinear regime, where clusters and constellation shape becomes distorted [37], [38].

Figure 5 shows a comparison of hard decision digital demodulation with k-means and EM demodulation. Numerical simulation was performed with a 960 km standard SMF link. A substantial improvement in the system performance in nonlinear regime for both both nonlinear phase noise-dominated link (Fig. 5(a)) as well as dispersion compensated link can be obtained (Fig. 5(b)). On the other hand, no improvement is observed for dispersion compensated link. Figure 6 presents constellations obtaned in respective cases from Fig. 5.

4. Conclusion

This paper reviews the architecture of a digital coherent receiver for optical communications. We describe the phys-
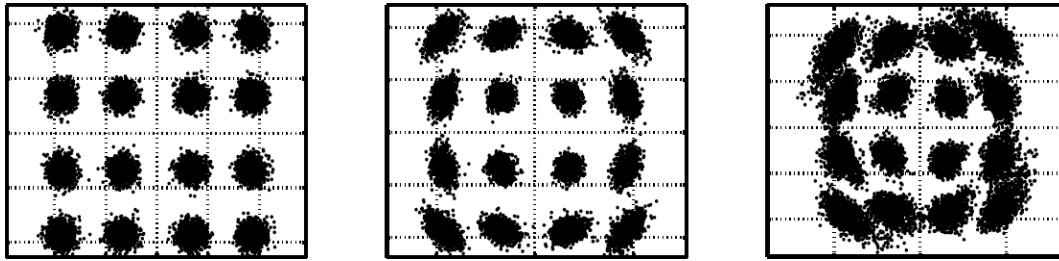
Fig. 4 Imprint of impairments on 16-QAM constellation. (a) Additive white Gaussian noise; (b) phase noise; (c) nonlinear phase noise.
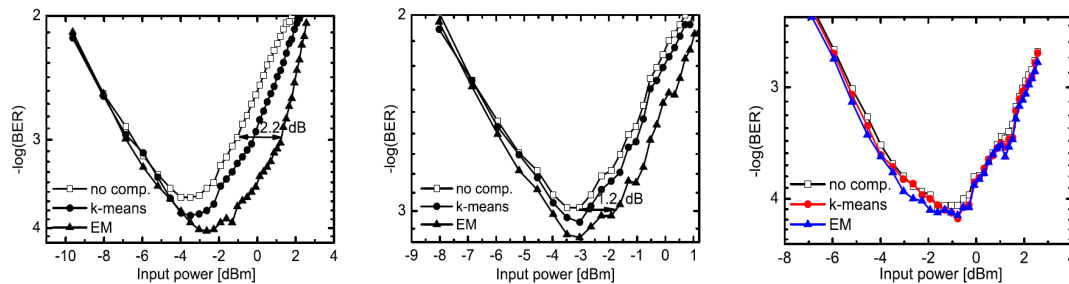
Fig. 5 Comparison of hard decision demodulation with k-means and EM demodulation for a 960 km transmission link. (a) Zero dispersion link dominated by nonlinear phase noise; (b) dispersion compensated link; (c) dispersion unmanaged link.
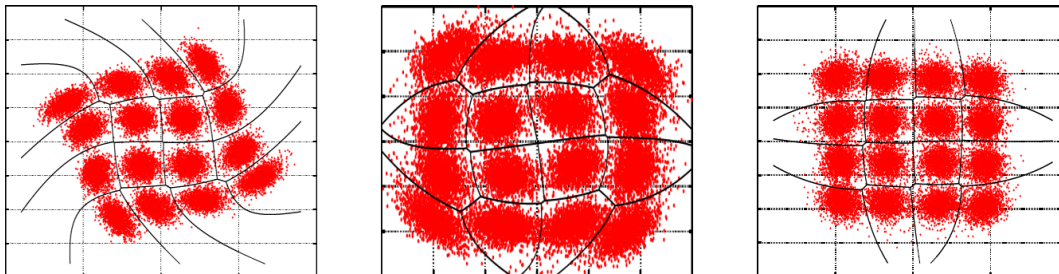
Fig. 6 Comparison of received constellation diagrams for: (a) zero dispersion link dominated by nonlinear phase noise (one span); (b) dispersion compensated link; (c) dispersion unmanaged link.

ical realization of the receiver, principle of coherent detection employed in the receiver, as well as digital signal processing algorithms that constitute its integral part. Due to very rapid development of electronics, real-time implementations of algorithms such as digital backpropagation or expectation maximization became possible just recently. Although the receivers being shipped to the market at present do not yet contain all of the functionalities presented here, it is clear that these advanced algorithms will become part of a coherent receiver sooner or later. Reconfigurable coherent transmitters and receivers are already commercially available. Algorithms, such as modulation format recognition or expectation maximization will lay foundations for next generation autonomous networks.

Acknowledgments

References

[1] R.J. Essiambre, G. Kramer, P.J. Winzer, G.J. Foschini, and B. Goebel, "Capacity limits of optical fiber networks," J. Lightwave Technol., vol.28, no.4, pp.662–701, Feb. 2010.

[2] S.J. Savory, "Digital coherent optical receivers: Algorithms and subsystems," IEEE J. Sel. Top. Quantum Electron., vol.16, no.5, pp.1164–1179, Sept. 2010.

[3] I. Tafur Monroy, D. Zibar, N.G. Gonzalez, and R. Borkowski, "Cognitive heterogeneous reconfigurable optical networks (CHRON): Enabling technologies and techniques," 2011 13th International Conference on Transparent Optical Networks, pp.1–4, June 2011.

[4] Optical Internetworking Forum, "Implementation Agreement for Integrated Dual Polarization Intradyne Coherent Receivers v01.2," 2013.

[5] M. Seimetz, High-Order Modulation for Optical Fiber Transmission (Springer Series in Optical Sciences), Springer, 2009.

[6] I. Fatadin, S.J. Savory, and D. Ives, "Compensation of quadrature imbalance in an optical QPSK coherent receiver," IEEE Photonics Technol. Lett., vol.20, no.20, pp.1733–1735, Oct. 2008.

[7] S.J. Savory, "Digital filters for coherent optical receivers," Opt. Express, vol.16, no.2, pp.804–817, Jan. 2008.

[8] X. Zhang, D. Zibar, I.T. Monroy, and R. Younce, "Engineering rules for chromatic dispersion compensation in digital receivers for optical coherent PolMux QPSK links," 2010 IEEE Photonic Society's 23rd Annual Meeting, pp.598–599, Nov. 2010.

[9] F.N. Hauske, J.C. Geyer, M. Kuschnerov, K. Piyawanno, T. Duthel, C.R. Fludger, D. van den Borne, E.D. Schmidt, B. Spinnler, H. de Waardt, and B. Lankl, "Optical performance monitoring from FIR filter coefficients in coherent receivers — OSA technical digest (CD)," Optical Fiber Communication Conference/National Fiber Optic Engineers Conference, OThW2, Optical Society of America, Feb. 2008.

[10] R. Borkowski, X. Zhang, D. Zibar, R. Younce, and I.T. Monroy, "Experimental adaptive digital performance monitoring for optical DP-QPSK coherent receiver," 37th European Conference and Exposition on Optical Communications, Washington, D.C., Tu.3.K.5, OSA, Sept. 2011.

[11] M. Kuschnerov, F.N. Hauske, K. Piyawanno, B. Spinnler, M.S. Alfiad, A. Napoli, and B. Lankl, "DSP for coherent single-carrier receivers," J. Lightwave Technol., vol.27, no.16, pp.3614–3622, Aug. 2009.

[12] D. Wang, C. Lu, A.P.T. Lau, and S. He, "Adaptive chromatic dispersion compensation for coherent communication systems using delay-tap sampling technique," IEEE Photonics Technol. Lett., vol.23, no.14, pp.1016–1018, July 2011.

[13] V. Ribeiro, S. Ranzini, J. Oliveira, V. Nascimento, E. Magalhães, and E. Rosa, "Accurate blind chromatic dispersion estimation in long-haul 112 Gbit/s PM-QPSK WDM coherent systems," Advanced Photonics Congress, Washington, D.C., SpTh2B.3, Optical Society of America, June 2012.

[14] Q. Sui, A.P.T. Lau, and C. Lu, "Fast and robust blind chromatic dispersion estimation using auto-correlation of signal power waveform for digital coherent systems," J. Lightwave Technol., vol.31, no.2, pp.306–312, Jan. 2013.

[15] F.C. Pereira, V.N. Rozental, M. Camera, G. Bruno, and D.A.A. Mello, "Experimental analysis of the power auto-correlation-based chromatic dispersion estimation method," IEEE Photonics Journal, vol.5, no.4, pp.7901608–7901608, Aug. 2013.

[16] F.N. Hauske, Z. Zhang, C. Li, C. Xie, and Q. Xiong, "Precise, robust and least complexity CD estimation," Optical Fiber Communication Conference/National Fiber Optic Engineers Conference 2011, Washington, D.C., JWA032, OSA, March 2011.

[17] R.A. Soriano, F.N. Hauske, N. Guerrero Gonzalez, Z. Zhang, Y. Ye, and I.T. Monroy, "Chromatic dispersion estimation in digital coherent receivers," J. Lightwave Technol., vol.29, no.11, pp.1627–1637, June 2011.

[18] C. Malouin, P. Thomas, B. Zhang, J. O'Neil, and T. Schmidt, "Natural expression of the best-match search godard clock-tone algorithm for blind chromatic dispersion estimation in digital coherent receivers," Advanced Photonics Congress, Washington, D.C., SpTh2B.4, OSA, June 2012.

[19] J.C. Diniz, S. Ranzini, V. Ribeiro, E. Magalhães, E. Rosa, V. Parahyba, L.V. Franz, E.E. Ferreira, and J. Oliveira, "Hardware-efficient chromatic dispersion estimator based on parallel gardner timing error detector," Optical Fiber Communication Conference/National Fiber Optic Engineers Conference 2013, Washington, D.C., OTh3C.6, OSA, March 2013.

[20] C. Malouin, M. Arabaci, P. Thomas, B. Zhang, T. Schmidt, and R. Marcoccia, "Efficient, non-data-aided chromatic dispersion estimation via generalized, FFT-based sweep," Optical Fiber Communication Conference/National Fiber Optic Engineers Conference 2013, Washington, D.C., JW2A.45, Optical Society of America, March 2013.

[21] E. Ip and J.M. Kahn, "Compensation of dispersion and nonlinear impairments using digital backpropagation," J. Lightwave Technol., vol.26, no.20, pp.3416–3425, Oct. 2008.

[22] F. Gardner, "A BPSK/QPSK timing-error detector for sampled receivers," IEEE Trans. Commun., vol.34, no.5, pp.423–429, May 1986.

[23] R. Borkowski, D. Zibar, A. Caballero, V. Arlunno, and I.T. Monroy, "Stokes space-based optical modulation format recognition for digital coherent receivers," IEEE Photonics Technol. Lett., vol.25, no.21, pp.2129–2132, Nov. 2013.

[24] C.M. Bishop, Pattern Recognition and Machine Learning (Information Science and Statistics), Springer, 2007.

[25] B. Szafraniec, B. Nebendahl, and T. Marshall, "Polarization demultiplexing in Stokes space," Opt. Express, vol.18, no.17, pp.17928–17939, Aug. 2010.

[26] Z. Yu, X. Yi, Q. Yang, M. Luo, J. Zhang, L. Chen, and K. Qiu, "Polarization demultiplexing in stokes space for coherent optical PDM-OFDM," Opt. Express, vol.21, no.3, pp.3885–3890, Feb. 2013.

[27] P. Serena, A. Ghazisaeidi, and A. Bononi, "A new fast and blind cross-polarization modulation digital compensator," European Conference and Exhibition on Optical Communication, Washington, D.C., We.1.A.5, Optical Society of America, 2012.

[28] N.J. Muga and A.N. Pinto, "Digital PDL compensation in 3D stokes space," J. Lightwave Technol., vol.31, no.13, pp.2122–2130, 2013.

[29] T. Saida, I. Ogawa, T. Mizuno, K. Sano, H. Fukuyama, Y. Muramoto, Y. Hashizume, H. Nosaka, and K. Murata, "In-band OSNR monitor for DP-QPSK signal with high-speed integrated stokes polarimeter," European Conference and Exhibition on Optical Communication, Washington, D.C., Th.2.A.2, Optical Society of America, 2012.

[30] R. Borkowski, X. Zhang, D. Zibar, R. Younce, and I.T. Monroy, "Experimental demonstration of adaptive digital monitoring and compensation of chromatic dispersion for coherent DP-QPSK receiver," Opt. Express, vol.19, no.26, pp.B728–B735, Dec. 2012.

[31] K. Kikuchi, "Polarization-demultiplexing algorithm in the digital coherent receiver," 2008 Digest of the IEEE/LEOS Summer Topical Meetings, pp.101–102, 2008.

[32] V.N. Rozental, T.F. Portela, D.V. Souto, H.B. Ferreira, and D.A.A. Mello, "Experimental analysis of singularity-avoidance techniques for CMA equalization in DP-QPSK 112-Gb/s optical systems," Opt. Express, vol.19, no.19, pp.18655–64, Sept. 2011.

[33] T. Pfau, S. Hoffmann, and R. Noe, "Hardware-efficient coherent digital receiver concept with feedforward carrier recovery for M-QAM constellations," J. Lightwave Technol., vol.27, no.8, pp.989–999, April 2009.

[34] D. Zibar, C. Peucheret, P. Jeppesen, and I. Monroy, "Digital coherent receiver for phase-modulated radio-over-fiber optical links," IEEE Photonics Technol. Lett., vol.21, no.3, pp.155–157, Feb. 2009.

[35] A. Viterbi, "Nonlinear estimation of PSK-modulated carrier phase with application to burst digital transmission," IEEE Trans. Inf. Theory, vol.29, no.4, pp.543–551, July 1983.

[36] F. Rice, M. Rice, and B. Cowley, "A new algorithm for 16QAM carrier phase estimation using QPSK partitioning," Digital Signal Process., vol.12, no.1, pp.77–86, 2002.

[37] D. Zibar, O. Winther, N. Franceschi, R. Borkowski, A. Caballero, V. Arlunno, M.N. Schmidt, N. Guerrero Gonzalez, B. Mao, Y. Ye, K.J. Larsen, and I.T. Monroy, "Nonlinear impairment compensation using expectation maximization for dispersion managed and unmanaged PDM 16-QAM transmission," Opt. Express, vol.20, no.26, B181, Nov. 2012.

[38] Y. Chen, C. Ruprecht, W. Rosenkranz, and N. Hanik, "Fiber nonlinearity compensation for dispersion unmanaged PDM 8-QAM CO-OFDM using expectation maximization," 18th OptoElectronics and Communications Conference, Kyoto, 2013.

Robert Borkowski received the M.Sc. Eng. and Ph.D. degrees from the Technical University of Denmark in 2011 and 2014, respectively. He is currently a postdoctoral researcher at the Department of Photonics Engineering, Technical University of Denmark. He has been actively involved in the European FP7 project CHRON (Cognitive Heterogeneous Reconfigurable Optical Network). Dr. Borkowski had been a visiting researcher at Centro de Pesquisa e Desenvolvimento em Telecomunicaes (CPqD) in Campinas, Brazil in 2012. His research interests are in the area of digital signal processing and machine learning for optical communications.

Darko Zibar was born on December 9th, 1978, in Belgrade, former Yugoslavia. He received the M.Sc. degree in Telecommunication in 2004 from the Technical University of Denmark and the Ph.D. degree in 2007 from the Department of Communications, Optics and Materials, COM•DTU within the field of optical communications. He was a Visiting Researcher with Optoelectronic Research Group led by Prof. John E. Bowers, at the University of California, Santa Barbara (UCSB) from January 2006 to August 2006, and January 2008 working on coherent receivers for phase-modulated analog optical links. From February 2009 until July 2009, he was Visiting Researcher with Nokia-Siemens Networks working on digital clock recovery for 112 Gb/s polarization multiplexed systems. Currently, he is employed at DTU Fotonik, Technical University of Denmark as the Assistant Professor. His research interests are in the area of coherent optical communication, with the emphasis on digital demodulation and compensation techniques. Darko Zibar is a recipient of the Best Student Paper Award at the IEEE Microwave Photonics Conference (MWP) 2006, for his work on novel optical phase demodulator based on a sampling phase-locked loop as well as Villum Kann Rasmussen postdoctoral research grant in 2007.

Idelfonso Tafur Monroy received the M.Sc. degree in multichannel telecommunications from the Bonch-Bruevitch Institute of Communications, St. Petersburg, Russia, in 1992, the Technology Licenciate degree in telecommunications theory from the Royal Institute of Technology, Stockholm, Sweden, in 1996, and the Ph.D. degree from the Eindhoven University of Technology, Eindhoven, The Netherlands, in 1999. He is currently a Professor and the Head of the Metro-Access and Short Range Communications Group, Department of Photonics Engineering, Technical University of Denmark, Lyngby, Denmark. In 1996, he joined the Department of Electrical Engineering, Eindhoven University of Technology, where he was an Assistant Professor until 2006. He has participated in several European research framework projects in photonic technologies and their applications to communication systems and networks. He is currently involved in the ICT European projects GigaWaMand EURO-FOS and is the Technical Coordinator of the ICT-CHRON project. His research interests include hybrid optical-wireless communication systems, high-capacity optical fiber communications, digital signal processing for optical transceivers for baseband and radio-over-fiber links, application of nanophotonic technologies in the metropolitan and access segments of optical networks as well as in short-range optical-wireless communication links.